The Disulfide Linkages and Glycosylation Sites of the Human Natriuretic Peptide Receptor-C Homodimer

John T. Stults,‡ Kathy L. O'Connell,‡ Chris Garcia,§ Stephen Wong,∥ Alfred M. Engel,⊥ David L. Garbers,∥,# and David G. Lowe*,⊥

Departments of Protein Chemistry, Molecular Biology, and Cardiovascular Research, Genentech, Inc., South San Francisco, California 94080, and Howard Hughes Medical Institute and Department of Pharmacology, University of Texas Southwestern Medical Center, Houston, Texas 75235

Received May 3, 1994; Revised Manuscript Received July 8, 1994®

ABSTRACT: The natriuretic peptide receptor-C (NPR-C) constitutes greater than 95% of the natriuretic peptide binding sites *in vivo*. This cell surface glycoprotein is a disulfide-linked homodimer with a subunit molecular weight of 68 000. Two sources and types of ANP affinity-purified human NPR-C were used to map disulfide linkages and glycosylation sites of this receptor by mass spectrometry: the extracellular domain obtained by papain cleavage of a receptor–IgG fusion protein expressed in Chinese hamster ovary cells, and a baculovirus/Sf9-expressed cytoplasmic truncation mutant in which 34 of 37 cytoplasmic domain amino acids were deleted. Two intramolecular disulfide bonded loops were found in the 435 amino acid extracellular domain (C63–C91, C168–C216). The juxtamembrane residues C428 and C431 are involved in homodimer formation, confirmed by site-directed mutagenesis of full-length NPR. Three of the four potential Asn-linked glycosylation sites are occupied: N41 (complex), N248 (high mannose), and N349 (complex; partial occupancy). These data describe the intra- and intermolecular linkages in NPR-C, providing a model for the homologous guanylyl cyclase receptors, NPR-A and NPR-B; both of the cyclase receptors likely contain the first amino-terminal 29 amino acid loop, but only NPR-A possesses the second 49 amino acid loop in common with NPR-C.

The natriuretic peptides are three related hormones termed atrial natriuretic peptide (ANP)[1] [reviewed by Brenner et al. (1990)], brain natriuretic peptide (BNP) (Sudoh et al., 1988), and C-type natriuretic peptide (CNP) (Sudoh et al., 1990). Both ANP and BNP are cardiac-derived vasorelaxants that stimulate natriuresis and diuresis (Brenner et al., 1990; Aburaya et al., 1989). ANP has been extensively characterized for its role in cardiovascular homeostasis as a direct and indirect antagonist to the renin/angiotensin/aldosterone system and to endothelin and vasopressin (Brenner et al., 1990; Ruskoaho, 1993). Both BNP and ANP are expressed by atrial myocytes and appear to have similar properties *in vivo*; however, BNP is expressed at a lower level than ANP, and expression by ventricular myocytes is greatly increased during hypertrophy (Mukoyama et al., 1991). In contrast, CNP is expressed by endothelial cells (Suga et al., 1992a) and is also a vasodilator (Sudoh et al., 1990), but may not play a significant role in natriuresis or diuresis (Stingo et al., 1992; Clavell et al., 1993) as a circulating hormone.

The natriuretic peptide receptors (NPRs) are a family of three homologous cell surface glycoproteins. Two of these receptors are membrane guanylyl cyclases called NPR-A or GC-A (Chinkers et al., 1989; Lowe et al., 1989), and NPR-B or GC-B (Chang et al., 1989; Schulz et al., 1989). For this class of receptor, hormone binding to the extracellular domain results in the direct production of the intracellular second messenger cGMP by the cytoplasmic catalytic domain. The receptor guanylyl cyclases are thought to mediate most or all of the biological responses to natriuretic peptides (Koller et al., 1991; Bennett et al., 1991; Suga et al., 1992b), but the third and much more abundant member of the natriuretic peptide receptor family is NPR-C, a non-guanylyl cyclase coupled receptor (Fuller et al., 1988) which *in vivo* comprises >95% of the binding sites for ANP, BNP, and CNP (Maack et al., 1993).

The two receptor guanylyl cyclases NPR-A and NPR-B share from 30% to 33% amino acid sequence identity with NPR-C in the extracellular domain. However, NPR-C only contains a 37 amino acid cytoplasmic domain compared to the large ~500 amino acid cytoplasmic domain for guanylyl cyclases. NPR-C appears to function in the internalization and degradation of bound natriuretic peptides (Nussenzveig et al., 1990) and is thought to contribute significantly to the short half-life (1–4 min) of ANP in plasma (Maack et al., 1993; Tan et al., 1993). In addition, however, numerous investigators have reported coupling of NPR-C to signal transduction pathways in tissue homogenates or cell lines [reviewed by Levin (1993)]. These pathways include stimulation of phosphatidylinositol hydrolysis (Hirata et al., 1989)

* To whom correspondence should be addressed.
‡ Department of Protein Chemistry, Genentech.
§ Department of Molecular Biology, Genentech.
∥ Department of Pharmacology, University of Texas Southwestern Medical Center.
⊥ Department of Cardiovascular Research, Genentech.
Howard Hughes Medical Institute.
® Abstract published in *Advance ACS Abstracts,* September 1, 1994.
[1] Abbreviations: NPR-A, natriuretic peptide receptor-A; NPR-B, natriuretic peptide receptor-B; NPR-C, natriuretic peptide receptor-C; ANP, atrial natriuretic peptide; BNP, brain natriuretic peptide; CNP, C-type natriuretic peptide; CHO, Chinese hamster ovary; DSS, disuccinimidyl suberate; ECD, extracellular domain; IgG, immunoglobulin G; C-IgG, NPR-C ECD/IgG Fc fusion protein; EDTA, ethylenediaminetetraacetic acid; EGTA, ethylene glycol bis(2-aminoethyl ether)-*N,N,N′,N′*-tetraacetic acid; HEPES, *N*-(2-hydroxyethyl)piperazine-*N′*-(2-ethanesulfonic acid); ACES, 2-[(carbamoylmethyl)amino]ethanesulfonic acid; PBS, phosphate-buffered saline; DFP, diisopropyl fluorophosphate; SDS–PAGE, sodium dodecyl sulfate–polyacrylamide gel electrophoresis; LC-MS, liquid chromatography–mass spectrometry; PMSF, phenylmethanesulfonyl fluoride; PNGase F, peptide-*N*-glycosidase F; DTT, dithiothreitol; TFA, trifluoroacetic acid; Fc, antibody complement-binding fragment; HexNAc, *N*-acetylhexosamine; NeuAc, *N*-acetylneuraminic acid.

0006-2960/94/0433-11372$04.50/0

and inhibition of adenylyl cyclase activity in a G_i-dependent pathway (Anand-Srivastava et al., 1987). The identity of NPR-C as mediating these signaling events is based principally on the apparent selectivity of ANP variants that do not bind to receptor guanylyl cyclases (Fuller et al., 1988).

NPR-C exists as a disulfide-linked homodimer on the cell surface (Schenk et al., 1987; Shimonaka et al., 1987); the mechanism and site of homodimer formation are not known, although membrane association may be important since soluble extracellular domain is secreted as a monomer (Porter et al., 1989). cDNA cloning has identified two different forms of NPR-C that differ by several amino acids, including an additional Cys residue (Fuller et al., 1988; Lowe et al., 1990; Porter et al., 1990). This difference is explained by the finding that alternate splicing generates nearly identical proteins with 5 (NPR-C5) or 6 (NPR-C6) cysteine residues (Mizuno et al., 1993), but both forms of NPR-C display similar kinetics of ligand binding and internalization (Mizuno et al., 1993).

We have previously expressed the cloned human NPR-C6 cDNA (Lowe et at., 1990) as an extracellular domain–IgG fusion protein (C-IgG) and characterized its binding properties (Bennett et al., 1991). In this report we used purified C-IgG as a source of receptor ECD to map the disulfide bonds and N-linked glycosylation sites by mass spectrometry. This information was then used to design mapping studies of purified homodimeric hNPR-C6 expressed using the baculovirus/Sf9 cell system. Two disulfide-linked loops in the NPR-C ECD and the site of receptor homodimer formation are defined. Mutagenesis studies of NPR-C Cys residues confirmed the juxtamembrane site of homodimer formation. Our results confirm and extend the work of Itakura et al. (1994) who have recently mapped the disulfide bonds of bovine NPR-C5. Furthermore, on the basis of sequence homology, we propose a model for the extracellular domain intramolecular disulfide linkages of the receptor guanylyl cyclases NPR-A and NPR-B.

EXPERIMENTAL PROCEDURES

C-IgG Cleavage and ECD Purification. The NPR-C ECD–IgG fusion protein (C-IgG) was secreted by CHO cells and purified as described previously (Bennett et al., 1991). Mercuripapain (Sigma) was used to cleave the IgG fusion protein in the hinge region and separate the Fc and the ECD portions from each other. To activate the papain, 20 μL (500 μg) of the mercuripapain ethanol slurry was centrifuged for 2 min at 10000*g* in an Eppendorf microcentrifuge. The supernatant was removed, and 1 mL of PBS, 20 mM EDTA, and 50 mM cysteine, pH 7.4, was added to resuspend the pellet. The papain solution was then incubated at 37 °C for 30 min with occasional resuspension. At the conclusion of the 30 min activation, the 1 mL papain solution was loaded onto a 5 mL Sephadex G-25 prepacked column (Bio-Rad) which had been preequilibrated with PBS and 5 mM EDTA, pH 7.4. Fractions (each 0.5 mL) were collected from the column, and A_{280} was measured for each to determine the papain-containing fractions. Peaks 3–5 contained the papain, and the concentration of protein was calculated using an extinction coefficient of 0.4 at 280 nm.

In preliminary experiments a time course for digestion and an optimum enzyme:substrate ratio were defined. The final digestion conditions used preactivated, desalted, thiol-free papain at an enzyme:substrate ratio of 1:1000 for 10 min in PBS with 5 mM EDTA at pH 7.4 and 37 °C. To digest the C-IgG, 17 mg of protein in 50 mL of PBS was prewarmed to 37 °C, and 17 μg of protein from the peak papain fraction was added with mixing. After 10 min, 0.5 mL of 5 M iodoacetamide (300 mM final concentration) was added to terminate the reaction. This was then incubated for an additional 15 min at 37 °C.

The 50 mL of digested fusion protein was loaded onto an ANP-Affi-gel column, prepared according to Meloche et al., (1988), at a flow rate of 0.3 mL/min. The flow-through was recycled twice. The column was then washed extensively with PBS prior to elution with 0.1 M sodium acetate and 1 M NaCl, pH 5.5. Fractions (0.5 mL) were collected and immediately neutralized with 1 M Tris, pH 8. ECD-containing fractions were determined by measuring A_{280}, and the amount of ECD was calculated assuming an extinction coefficient of 1.0. The final total yield of NPR-C ECD was 4 mg, which was concentrated by vacuum dialysis to 10 mg/mL in 20 mM HEPES and 50 mM NaCl, pH 7.2.

NPR-C Expression in Sf9 Cells and Purification. The full-length NPR and cytoplasmic domain-truncated human NPR-C6Δ34 cDNA (Lowe et al., 1990) was cloned into the baculovirus expression vector pVL-1392 (Pharmingen). The vector was cotransfected with AcRP23-LAZ (Possee & Howard, 1987) into Sf9 cells, and the recombinant virus was cloned according to Kitts et al. (1990). Sf9 cells infected with the recombinant virus expressed up to 6 pmol of ^{125}I-ANP binding site/mg in crude particulate fractions, while no significant binding was detected from uninfected Sf9 cells.

NPR-C was solubilized as follows: 60 h postinfection with recombinant virus, Sf9 cells were frozen in liquid nitrogen. The frozen pellets were thawed in the presence of 50 mM Tris-HCl, pH 7.5, 100 mM NaCl, 10% glycerol, 1 mM EDTA, 10 mg/mL leupeptin, 20 mg/mL aprotinin, 2 mg/mL pepstatin, 0.4 mM PMSF, and 0.1 mM DFP. The thawed cells were disrupted with a Dounce homogenizer, and crude particulate fractions were obtained and washed by centrifugation in the same buffer. The particulate fraction was rocked for 60 min at 4 °C in the above buffer containing 1% digitonin and 0.2% cholate. Detergent extract containing NPR-C was obtained by centrifugation at 100000*g* and was diluted 10-fold with the same buffer without detergent. $MgCl_2$ was then added to a final concentration of 10 mM. Approximately 80% of the ^{125}I-ANP binding activity in the particulate fraction was solubilized.

Purification of NPR-C was performed as follows: the detergent extract was loaded to an ANP–agarose column which was prepared according to Meloche et al. (1988). The column was first washed with 50 mM HEPES, pH 7.5, 10% glycerol, 0.0125% phosphatidylcholine, 0.1% Lubrol 12A9, 1 mM EGTA, 10 mM $MgCl_2$, 10 mg/mL leupeptin, 20 mg/mL aprotinin, 2 mg/mL pepstatin, 0.4 mM PMSF, 0.1 mM DFP, 0.5 mg/mL bacitracin, and 150 mM NaCl. The column was then washed sequentially with the same buffer with 1 M NaCl, and then with buffer without NaCl. NPR-C was eluted by mixing the gel with 50 mM sodium acetate, pH 5.5, 1 M NaCl, 0.1% lubrol 12A9, 20% glycerol, 0.025% phosphatidylcholine, and 0.5 mM EDTA and eluting by gravity flow. The eluted fraction was immediately neutralized with an equal volume of 1 M HEPES, pH 7.5. Typical yield of the purification is about 90–95%, with no detectable contaminants observed in silver staining of the purified fraction after SDS–PAGE (data not shown). Approximately 50% of the purified NPR-C6 and 90% of NPR-C6Δ34 was obtained in its nonreduced, dimeric form.

Tryptic Digestion of Purified NPR-C. Trypsin (0.05 μg, Promega, Modified) was added to purified ECD (90 pmol in 20 μL of 100 mM ammonium bicarbonate, pH 7.8). The solution was incubated at 37 °C. After 12 h, an additional

0.1 μg of trypsin was added and the digestion continued for another 12 h. The reaction was stopped by freezing the solution at −20 °C.

In a separate reaction, the peptide digest was deglycosylated and reduced. Following trypsin digestion as described above, the reaction was stopped by addition of 0.5 μL of PMSF in 2-propanol. After 50 min at room temperature, 8 μL of PNGase F (2 units, Genzyme, glycerol-free) and 5 μL of 100 mM EDTA were added and the reaction proceeded for 24 h at 37 °C. The peptides were reduced subsequently by addition of 20 μL of 1 M DTT, followed by further incubation at 37 °C for an additional 10 min.

To minimize potential disulfide rearrangement, another tryptic digest was performed at pH 7. To 1 nmol of purified ECD in 10 mM ACES and 20 mM $CaCl_2$, pH 7.0, was added 0.25 μg of trypsin, followed by incubation at 37 °C for 4 h. A second 0.25 μg aliquot of trypsin was added, and the incubation was continued for 4 h more. The reaction was stopped by freezing at −20 °C.

Before tryptic digestion, the NPR-C6Δ34 (100 pmol) was dialyzed against 7 M urea at 4 °C for 72 h to remove the detergent. The volume was reduced to 10 μL by ultracentrifugation with a Microcon Concentrator (10-kDa cutoff, Amicon). The solution was diluted to 2 M urea with 100 mM ammonium bicarbonate, and the tryptic digestion was performed as described above at pH 7.8.

Liquid Chromatography–Mass Spectrometry. The HPLC system consisted of an Applied Biosystems 140A dual-syringe pump that was operated at 100 μL/min. The solvent flow was split to 3–4 μL/min with a tee-union (Valco); the split ratio was set by a length of 75 μm fused silica capillary tubing (Polymicro Technologies) attached to the tee. The other arm of the tee was attached through a short piece of capillary to an injection valve (Rheodyne) with a 20 μL sample loop. The C18 packed capillary column (0.32 × 100 mm) (LC Packings) was attached directly to the injector. The exit of the column was attached via a short piece of capillary tubing to the electrospray needle. Solvent A was 2% acetonitrile/0.05% TFA. Solvent B was 90% acetonitrile/0.0425% TFA. After injection, the column was washed at 0% B for 30 min, followed by peptide elution with a 0–60% B gradient in 60 min. Alternatively, a 0.180 × 100 mm C18 column was used, in which case the solvent flow was split to 2 μL/min.

Larger scale separation was performed with a UMA HPLC system (Michrom BioResources, Inc.) using a 1.0 × 150 mm C18 column. The flow rate was 50 μL/min with solvent composition and gradient identical to that given above. The effluent stream was split after the UV detector to feed approximately 5 μL/min into the mass spectrometer. The remainder was diverted to a fraction collector.

A PE-Sciex API *III* triple-quadrupole mass spectrometer with an Ionspray source was used for all LC-MS experiments. Spectra for the ECD digest were acquired in the mass range of 500–2000 u with a 0.25 u step, 1 ms dwell time. The NPR-C6Δ34 digest spectra were acquired in the range of 400–2000 u with a 0.33 u step. At the beginning of each scan, oxonium ions that are characteristic fragments of carbohydrates (m/z 204.1 for $HexNAc^+$, m/z 292.1 for $NeuAc^+$, and m/z 366.1 for $HexHexNAc^+$) were monitored at elevated orifice potential (160 V) (Conboy & Henion, 1992; Huddleston et al., 1993). This in-source dissociation technique makes possible the rapid identification of both N-linked and O-linked peptide glycosylation. Data were acquired with the TUNE program (Sciex) in the MIM mode, with 6 u windows for m/z 204.1, 292.1, and 366.1 (at OR = 160 V), and a 1600 u window centered at m/z 1200 (at OR = 80 V). Data were interpreted with the aid of MAPMASS, a program developed to match expected peptide masses with the observed masses.

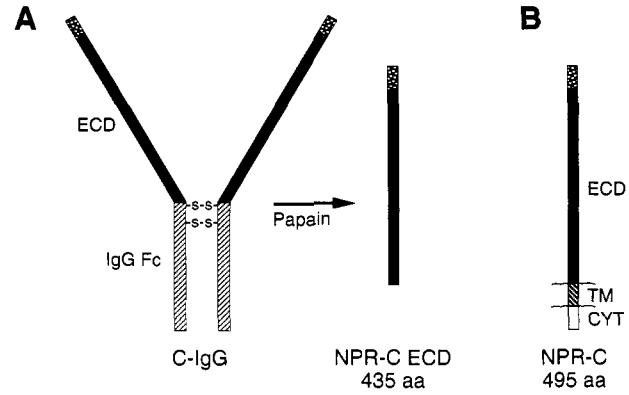

FIGURE 1: Diagram of two forms of NPR-C used for structural studies. (*A*) Model of the C-IgG dimer with disulfide bonds in the hinge region of the IgG heavy chain. Cleavage with papain in the hinge region was followed by purification of the 435 amino acid ECD by ANP affinity chromatography (see Experimental Procedures). (*B*) Structure of the NPR-C monomer showing the 442 amino acid extracellular domain, transmembrane domain, and the 37 amino acid cytoplasmic domain. In both (*A*) and (*B*), a heterogeneous amino terminus due to incomplete processing of a glycine-rich segment is indicated by a stippled box.

Protein N-Terminal Sequencing. Approximately 5 pmol of protein, separated by SDS–PAGE, was electroblotted (Matsudaira, 1987) onto an Immobilon-PSQ membrane (Millipore). HPLC-purified tryptic disulfide-linked peptides were spotted on a membrane. The samples were sequenced with an ABI 477 protein sequencer (Applied Biosystems).

ANP Cross-Linking to Cys Mutants. Site-directed mutagenesis of human full-length NPR-C was performed by the method of Kunkel (1985) using the Bio-Rad (Hercules, CA) phagemid kit. Human 293 cells were transfected by $CaCl_2$ coprecipitation (Gorman et al., 1990) with wild-type and cysteine-mutated receptors. After 3 days the plates were washed with PBS and 0.5% BSA and subsequently incubated in the same buffer supplemented with 50 pmol of ^{125}I-ANP. After 1 h the bifunctional cross-linker disuccinimidyl suberate was added to a final concentration of 2 mM and incubated for another 30 min. All procedures were performed on ice to prevent internalization and degradation of the ligand. Finally, the incubation mixture was removed, and the cells were lysed by adding SDS–PAGE sample buffer.

RESULTS AND DISCUSSION

The NPR-C is a disulfide-linked homodimer in which each monomeric subunit consists of a 435 (C6) or 436 (C5) amino acid, glycosylated extracellular domain (ECD), a single transmembrane domain, and a 37 amino acid cytosolic domain. A membrane-targeting signal sequence and 22 amino acid glycine-rich segment are cleaved to yield the mature wild-type protein. Two constructs of the receptor were characterized. Initially, the extracellular domain (ECD) from an IgG fusion protein (Figure 1A) (Bennett et al., 1991) was prepared. For this chimeric form of the receptor, the ECD was cleaved from the Fc segment by papain digestion, and the purified ECD was recovered by ligand affinity chromatography on an ANP column. This protein was readily available in adequate quantity for development of the methods used here; its binding characteristics were known (Bennett et al., 1991; Engel et al., 1994), and glycosylation patterns similar to the wild-type

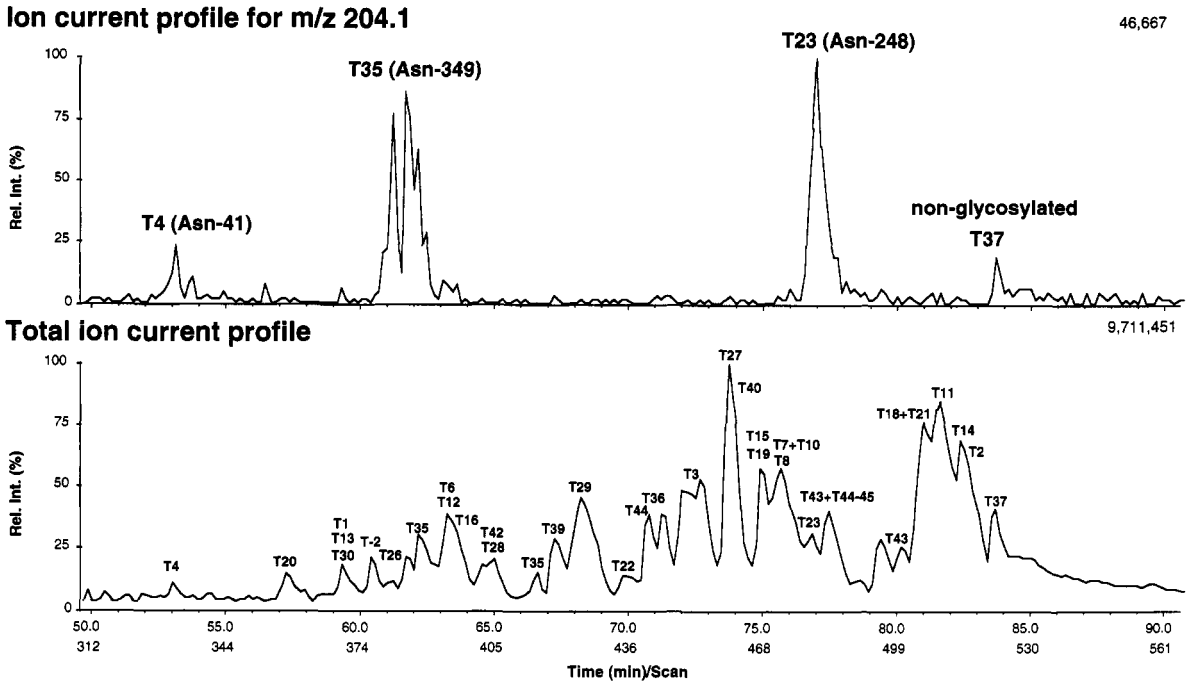

FIGURE 2: Fragment ion and total ion current chromatograms. Glycopeptides are identified by oxonium fragment ion (derived from GlcNAc) intensity from m/z 204.1 (upper trace) that was produced by in-source collisional activation (see Experimental Procedures). Peptide T37 coincidentally displays a fragment ion at m/z 204.1 but is not glycosylated. The total ion current (TIC) chromatogram for the nonreduced trypsin digest of the ECD is shown in the lower trace. The data were generated by capillary HPLC electrospray ionization mass spectrometry. The peptide identities are given in Table 1.

human protein were expected. The second form of the receptor studied was NPR-C6 (Figure 1B) expressed in insect Sf9 cells infected with recombinant baculovirus.

Mass spectrometric methods were used for most of the molecular characterization. Mass spectrometry has been used extensively for protein characterization [as reviewed by Carr et al. (1991)], including disulfide assignment (Morris & Pucci, 1985), and it offers a rapid means to identify most of the components in a proteolytic map. Furthermore, it has become the method of choice for the identification of glycosylation sites (Carr & Roberts, 1986; Ling et al., 1991; Conboy & Henion, 1992; Huddleston et al., 1993).

Characterization of the Extracellular Domain. Amino-terminal sequencing of the affinity-purified NPR-C ECD yielded two sequences (TGGGGVGGGGGGAGIGGG and EALPPQKIEVLVLLPQDD) of approximately equal abundance as previously observed for the IgG fusion protein (Bennett et al., 1991). The first sequence results from signal peptidase cleavage of the precursor, and the second from a trypsin-like cleavage that is 22 residues downstream. The molecular mass of approximately 50 kDa, determined by SDS–PAGE (data not shown), for either the reduced or nonreduced protein is in general agreement with the mass expected for the core polypeptide (exclusive of carbohydrate, expected M_r = 49 605 for the wild-type N-terminus, 51 358 including the glycine-rich N-terminal segment). The ECD derived from the fusion protein exists solely as a monomer, in contrast to the wild-type receptor that is observed to be predominantly a homodimer. According to the model of the C-IgG fusion protein (Figure 1), this molecule is a dimer via linkage at the hinge region of the Fc domain. The Fc portion may prevent native dimerization of the NPR-C6 ECD by holding the two subunits in a configuration that does not permit proper interchain disulfide bonding. Nonetheless, the dimeric fusion protein binds ANP with high affinity (Bennett et al., 1991). Furthermore, the monomeric ECD is sufficient for binding ANP (Porter et al., 1989) as evidenced by the receptor's purification with an ANP affinity column. These data also demonstrate that the glycine-rich segment at the amino terminus of NPR-C does not impair ligand binding.

LC-MS Analysis of the ECD. The nonreduced ECD was digested with trypsin, and the tryptic map was characterized by LC-MS. Figure 2 shows the total ion current (TIC) chromatogram for the tryptic map. The identities of the peptides and their observed masses are given in Table 1. The resolution of the mass spectrometer was sufficient to show isotope peak separation for singly-charged peptides. The mass assignments were of sufficient accuracy to show deamidation of one of the peptides (T_{36}) that contains a site that is a likely candidate for deamidation (Asn-Gly). The extent of the entire sequence that was mapped in this experiment (86%) is shown in Figure 3.

Two of the peptides observed in the spectra from the nonreduced ECD correspond in mass to disulfide-linked peptides, T7+T10 and T18+T21 (see Table 1). These peptides show two of the disulfide bonds as Cys63–Cys91 and Cys168–Cys216. None of these four peptides were observed as free thiols. The two disulfide-linked peptides were not observed in the tryptic map of reduced ECD, whereas three of four of the corresponding free cysteine-containing peptides (T7, T10, and T21) were observed for the reduced protein (data not shown). A peptide (T43+T44-45) was also observed in the tryptic map of the nonreduced ECD that corresponds to disulfide bonding of Cys428–Cys431. This peptide was not observed in the map of the reduced protein; only T43 was observed in the reduced protein digest. Peptides that correspond in mass to the free thiols of Cys428 (T43) and Cys431 (T44) were also observed in the nonreduced protein, but at different retention times than the disulfide-linked peptide, a suggestion of partial disulfide bonding of these two peptides. Examination of the data for all other possible combinations of cysteines revealed no other intrachain disulfide bonds.

In order to reduce the possibility of disulfide shuffling that may occur at basic pH, the digest was repeated at pH 7.0.

Table 1: Masses Observed for the Tryptic Map of the ECD and NPR-C6Δ34

tryptic peptide	amino acid from:	amino acid to:	expected mass (Da)	observed mass[a] (Da) ECD NPR-C	observed mass[a] (Da) NPR-C6Δ34
ECD					
T(−2)	−22	−2	1356.6	1356.6	1356.7
T(−1)	−3	−1	431.2		
T1	1	7	781.4	781.4	
T2	8	26	2221.6a	2221.6a	2221.8a
T3	27	36	1187.4a	1187.6a	1187.4a
T4	37	45	875.4	*b*	
T5	46	46	174.1		
T6	47	53	752.4	752.5	752.5
T7	54	66	1503.6a	*c*	*c*
T8	67	74	919.5	919.7	919.5
T9	75	79	486.3		486.4
T10	80	100	2111.5a	*c*	*c*
T11	101	122	2321.7a	2321.3a	2321.5a
T12	123	131	1106.5	1106.5	1106.6
T13	132	138	718.4	718.4	718.5
T14	139	148	1197.6	1197.6	
T15	149	154	858.4	858.4	
T16	155	163	980.5	980.6	
T17	164	166	416.2		
T18	167	195	3423.7a	*c*	
T19	196	204	1086.6	1086.6	1086.6
T20	205	211	816.4	816.4	
T21	212	223	1294.6a	*c*	
T22	224	231	925.5	925.7	925.5
T23	232	258	3018.2a	*b*	
T24	259	259	174.1		
T25	260	262	318.2		
T26	263	268	745.3	745.4	
T27	269	281	1479.7a	1479.5a	1479.7a
T28	282	289	976.5	976.5	976.3
T29	290	295	739.4	739.4	739.3
T30	296	300	548.3	548.5	
T31	301	332	3750.3a		3782.1[e]
T32	333	337	524.3		524.7
T33	338	338	146.1		
T34	339	342	375.2		
T35	343	350	1058.2a	1058.0a[d]	*b*
T36	351	367	1748.8	1749.8[f]	
T37	368	393	2813.1a	2813.0a	2812.7a
T38	394	396	360.2		
T39	397	404	1020.2a	1020.0a	1020.a
T40	405	411	859.5	859.4	859.5
T41	412	413	287.2		
T42	414	418	645.3	645.3	
T43	419	429	1213.6	1213.6	*c*
T44	430	440	1167.2a	1167.3a	
T45	441	442	256.3a	*c*	
T7+T10[g]			3613.0a	3613.0a	3612.9a
T18+T21[g]			4716.3a	4716.4a	
T43+t44–45[g]			2617.9a	2618.9a	
NPR-CΔ34					
T44	430	459	3092.7a		*c*
T45	460	460	146.2a		*c*
T46	461	461	146.2a		*c*
T43+T44-46[g]			4561.4a		4561.0a

[a] Masses given are monoisotopic when isotope peaks are discernible; otherwise, they are the isotopically averaged mass designated by "a". [b] Fully glycosylated. [c] Observed only as disulfide-bonded peptide. [d] Partially glycosylated. [e] Observed doubly oxidized. [f] Deamidated peptide. [g] "+" indicates disulfide-bonded peptides; a "-" indicates incomplete tryptic cleavage.

Disulfide shuffling has been shown not to occur in other proteins when digested with trypsin at neutral pH (Gall et al., 1968). The T7+T10 and T18+T21 peptides were observed; however, no peptides were observed in this experiment to contain Cys428 and Cys431, either as free sulfhydryls or in disulfide linkage. No masses were observed that correspond to interchain disulfide bonds. For this latter experiment, a larger bore HPLC column was used and the column flow was split so that a fraction of the effluent was sent to the mass spectrometer and the remainder was recovered in a fraction collector. Automated Edman degradation of the fractions that contained the disulfide-linked peptides (T7+T10, T18+T21) confirmed their sequences (data not shown). The T18+T21 peptide in particular was hydrophobic and required a higher concentration of acetonitrile (50%) in order to be removed from the fraction collection tube for sequencing.

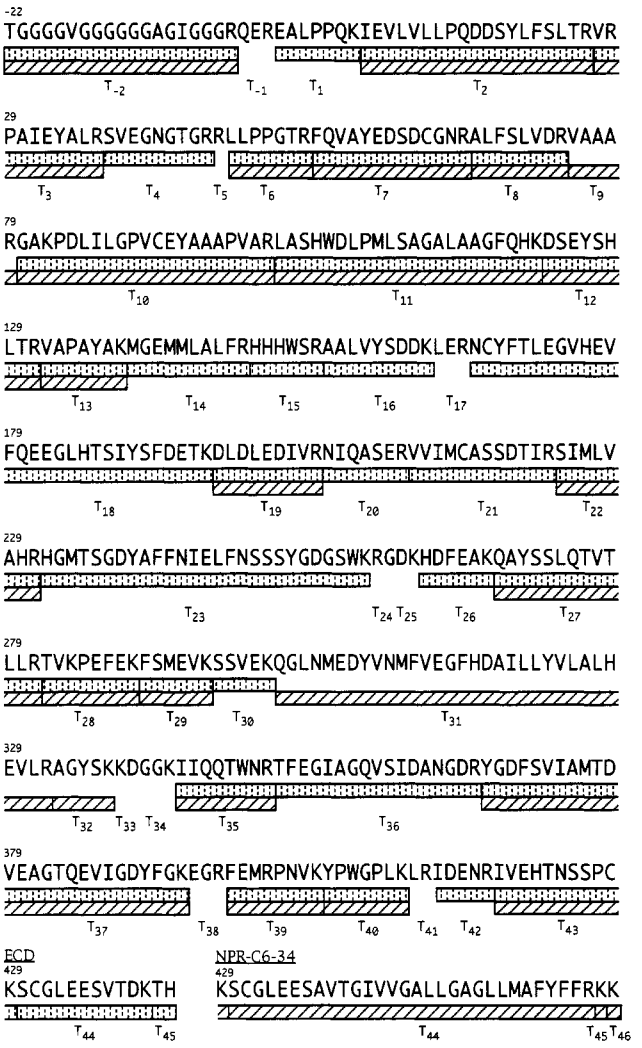

FIGURE 3: Extent of NPR-C mapped by mass spectrometry. The amino acid sequence of human NPR-C6 is shown in single-letter amino acid code. Numbering is based on the sequence of the mature wild-type receptor. Tryptic fragments identified by LC-MS from the C-IgG-derived ECD are indicated by a stippled bar, and fragments from the NPR-C6Δ34 are in a hatched bar.

Approximately 15% of the peptides found in the TIC (Figure 2) were not readily assigned to expected tryptic fragments of the ECD. A peak in the TIC that corresponds to T27 also includes a component that is 17 u lower in mass than T27. An N-terminal glutamine is present in T27; thus this component is likely the pyroglutamic acid form of T27. Pyroglutamic acid could be formed during the digestion and/or the subsequent separation in acidic solvents (Blomback, 1967). No other post-translational modifications besides glycosylation were evident from the tryptic map. Most of the unidentified peaks appear to arise from nonspecific cleavage by trypsin during the 24 h incubation. In contrast, the pH 7.0 trypsin digest (see above) was terminated at 8 h (rather than at 24 h as for the pH 7.8 digestion), and the LC-MS tryptic map produced fewer unassigned peptides; however, significant

Table 2: Identified Carbohydrate Structures

tryptic peptide	glycoslyation		expected mass (Da)	observed mass (Da)
ECD NPR-C				
T4 (Asn41)	$Hex_3HexNAc_3DeoxyHex_1$	(incomplete biantennary)[a]	2118.0	2117.6
	$Hex_3HexNAc_4DeoxyHex_1$	(incomplete biantennary)	2321.2	2320.6
	$Hex_4HexNAc_4DeoxyHex_1$	(incomplete biantennary)	2483.4	2483.1
	$Hex_5HexNAc_4DeoxyHex_1$	(asialobiantennary)	2645.5	2644.9
	$NeuAc_1Hex_4HexNAc_4DeoxyHex_1$	(incomplete biantennary)	2774.6	2774.6
	$NewAc_1Hex_5HexNAc_4DeoxyHex_1$	(monosialobiantennary)	2936.8	2937.0
	$NeuAc_2Hex_5HexNAc_4DeoxyHex_1$	(disialobiantennary)	3228.0	3227.5
T23 (Asn248)	$Hex_4HexNAc_2$	(Man_4 high mannose)	4073.2	4072.6
	$Hex_5HexNAc_2$	(Man_5 high mannose)	4235.3	4234.7
	$Hex_6HexNAc_2$	(Man_6 high mannose)	4397.5	4398.0
	$Hex_7HexNAc_2$	(Man_7 high mannose)	4559.6	4559.6
	$Hex_8HexNAc_2$	(Man_8 high mannose)	4721.7	4722.6
	$Hex_9HexNAc_2$	(Man_9 high mannose)	4883.9	4883.9
T35 (Asn349)	$NeuAc_1Hex_4HexNAc_4DeoxyHex_1$	(incomplete biantennary)	2957.0	2955.6
	$NeuAc_1Hex_5HexNAc_4DeoxyHex_1$	(monosialobiantennary)	3119.1	3119.2
	$NeuAc_2Hex_5HexNAc_4DeoxyHex_1$	(disialobiantennary)	3410.4	3410.6
	$NeuAc_2Hex_6HexNAc_5DeoxyHex_1$	(disialotriantennary)	3775.7	3775.9
	$NeuAc_3Hex_6HexNAc_5DeoxyHex_1$	(trisialotriantennary)	4067.0	4066.6
	$NeuAc_3Hex_7HexNAc_6DeoxyHex_1$	(trisialotetraantennary)	4432.3	4432.7
	$NeuAc_4Hex_7HexNAc_6DeoxyHex_1$	(tetrasialotetraantennary)	4723.6	4723.8
T43 (Asn424)	not observed			
NPR-C6Δ34				
T4	not observed			
T23	not observed			
T35	$Hex_5HexNAc_2$	(Man_5 high mannose)	2275.3	2274.2
	$Hex_6HexNAc_2$	(Man_6 high mannose)	2437.4	2436.6
	$Hex_7HexNAc_2$	(Man_7 high mannose)	2599.6	2599.2
	$Hex_8HexNAc_2$	(Man_8 high mannose)	2761.7	2762.2
T43	not observed			

[a] Predicted glycoform based upon known mammalian carbohydrate structures for the ECD NPR-C, and insect structures for the NPR-C6Δ34.

partial digestion was evident from additional peptides in the 4–6 kDa range, and a smaller fraction of the sequence (72%) was mapped in that experiment.

Glycosylation Sites for the ECD. The Asn-linked glycosylation sites were also identified by tryptic mapping with LC-MS. Peptides were observed in the tryptic map that correspond in mass to three of four potential N-linked sites plus carbohydrate (positions 41, 248, and 349) (see Table 2). The first two sites, Asn41 and Asn248, appear to be fully glycosylated. A peptide was observed for the nonglycosylated T35; thus the Asn349 site appears to be partially glycosylated. The mass of the carbohydrate moiety on each peptide is sufficient for determination of the oligosaccharide composition, i.e., the number of *N*-acetylneuraminic acid, hexose, *N*-acetylhexosamine, and deoxyhexose monosaccharides. The identified carbohydrate compositions are given in Table 2 for each potential Asn-linked site. On the basis of the known Asn-linked structures from CHO cells (Spellman et al., 1989), the monosaccharides present are assumed to be *N*-acetylneuraminic acid, mannose, galactose, *N*-acetylglucosamine, and fucose. Only the *N*-acetylneuraminic acid mass uniquely defines the monosaccharide. No further structural studies of the carbohydrates were undertaken to confirm these structures nor to provide any data on branching or linkage.

The Asn41 site consisted of seven biantennary complex carbohydrate structures including smaller, incompletely processed structures. The monosialobiantennary glycoform corresponding to mass 2937.0 Da was the most abundant. The Asn248 position contained six high-mannose structures ranging from four to nine mannoses, with $Man_9GlcNAc_2$ (glycopeptide mass 4883.9 Da) observed as the most abundant. The Asn349 site contained seven biantennary, triantennary, and tetraantennary complex structures. The disialobiantennary structure was present as the most abundant glycoform followed by the monosialobiantennary structure (glycopeptide masses 3410.6 and 3119.2 Da, respectively). No glycosylation was observed for Asn424. No evidence of O-linked oligosaccharides was observed in the ECD.

The glycosylation sites were confirmed by three methods. First, carbohydrate heterogeneity results in distinctive diagonal patterns of ion abundance in a contour plot of the data (Ling et al., 1991). The diagonal patterns appear because larger carbohydrate structures elute slightly earlier in reversed-phase HPLC due to greater hydrophilicity, and they appear at higher mass than the same peptide with a smaller carbohydrate structure. These diagonal patterns were observed for the ECD glycopeptides (data not shown). Second, glycopeptides yield fragment oxonium ions that are characteristic of carbohydrates. These fragment ions arise from in-source collisional activation in an electrospray ion source (Conboy & Henion, 1992; Huddleston et al., 1993). The ions monitored during the tryptic mapping of the ECD were m/z 204.1 ($HexNAc^+$), 292.1 ($NeuAc^+$), and 366.1 ($HexHexNAc^+$). The reconstructed ion current profile for m/z 204.1 is shown in Figure 2. The three glycopeptides are clearly identified by the three peaks in the profile. The peak splitting observed in the m/z 204.1 profile for T35 corresponds to different, partially separated glycoforms. The m/z 204.1 signal for T37 represents a non-carbohydrate fragment for this peptide. [The y_2 fragment for T37, which corresponds to two amino acids at the C-terminus, GK, appears at m/z 204.1. Peptide fragmentation nomenclature is described in Johnson et al. (1987).] Third, the tryptic map was repeated after removal of Asn-linked carbohydrate by PNGase F digestion. Treatment with PNGase F increases the retention time of the previously glycosylated peptide, and the mass of the peptide reflects loss

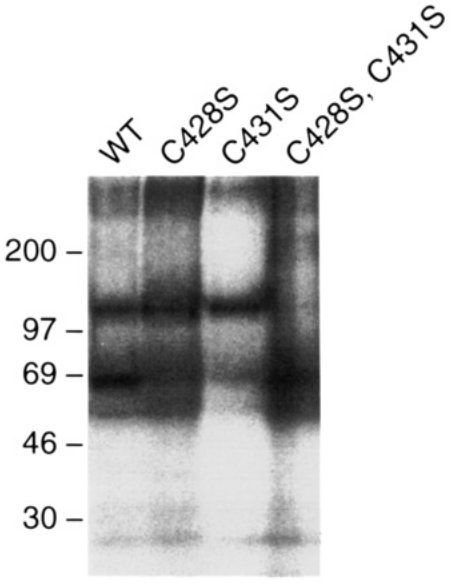

FIGURE 4: Cross-linking of ^{125}I-hANP to NPR-C. Human 293 cells were transfected with NPR-C6 ("WT") and mutants changing either one of the two juxtamembrane Cys residues to Ser ("C428S" and "C431S"), or both together ("C428S, C431S"). Transiently expressed receptors were cross-linked with ^{125}I-ANP using DSS, and nonreduced samples were analyzed by SDS–PAGE and visualized with a phosphorimager (Fuji Biosystems). Molecular weight standards are shown on the left.

of the carbohydrate and conversion of Asn to Asp (Carr & Roberts, 1986). The trypsin- and PNGase-digested ECD yielded the appropriate mass- and retention time-shifted peptides for the three glycosylation sites (data not shown).

Characterization of the Truncated Receptor. The full-length NPR-C6 was expressed in Sf9 cells as was a truncated version of the receptor in which 34 of 37 amino acids of the cytosolic domain were deleted (Δ34). Both receptors exist as monomers and disulfide-linked dimers (data not shown), demonstrating that the cytoplasmic domain of the receptor is not required for homodimer formation. Only the truncated receptor was extensively characterized by mass spectrometry, due to the limited availability of the full-length receptor. The hydrophobic nature of the additional transmembrane region in these receptors, as compared to the ECD, resulted in greater sample losses during handling. Mass spectrometric analysis requires the complete removal of detergent, which may be responsible for much of the sample loss. Edman sequencing of the NPR-C6Δ34 gave two sequences that correspond to amino termini at residues –22 (95% TGGGGVGGGGGGA) and –19 (5% GGVGGGGGGAGIG).

LC-MS Analysis of NPR-C6Δ34. The nonreduced truncated receptor was digested with trypsin, and the tryptic map was characterized by LC-MS. The observed masses are given in Table 1. The capillary column used for this map (180 μm) was smaller than the column that had been used for the map of the ECD (320 μm). Nonetheless, the elution order of the peptides was nearly identical to the tryptic map of the ECD. Overall, the signal was weaker and the number of expected peptides that were observed is smaller. The extent of the sequence that was mapped in this experiment is shown in Figure 3 along with the results presented earlier for the ECD tryptic map.

A peptide was observed that indicates that the first pair of cysteines are linked (Cys63–Cys91). No signal was observed for the second pair of cysteines that had been observed to be linked in the ECD. The limited solubility of the Cys168–Cys216 peptide in the ECD (see above) may explain its absence. A peptide was also observed that corresponds to linkage of the last two cysteines (Cys428–Cys431). This peptide could represent either an intramolecular or intersubunit disulfide bond. These two possibilities could not be distinguished by mass or sequence in this experiment since the monomer and dimer forms of NPR-C6Δ34 were not separated before analysis. No other cysteine-containing peptides were observed that correspond either to free sulfhydryls or to any other disulfide linkages.

Glycosylation Sites for NPR-C6Δ34. The Asn-linked glycosylation sites were also determined from the LC-MS data. Monitoring the oxonium ion masses that result from in-source collisional activation showed a single, low-abundance peak for both m/z 204.1 and 366.1 that matched T35 (Asn349). The masses of the T35 glycoforms suggest all simple high-mannose structures (see Table 2) which are known to be synthesized in insect cell lines (Manneberg et al., 1994). The most abundant glycoform was $Man_6GlcNAc_2$ (glycopeptide mass 2436.6). No signal was observed for nonglycosylated T35; thus this site appears to be fully glycosylated. Peptides that contain Asn41 or Asn248 were not observed. The lack of a signal for the oxonium ion at m/z 204.1 suggests that these peptides were not glycosylated, but the absence of a signal for the nonglycosylated peptide does not confirm this result. The peptide that contains Asn424 was observed only without carbohydrate. It thus appears that the protein is less heavily glycosylated by the insect cells than by mammalian cells, an observation that has been made for other glycoproteins (Goochee et al., 1991).

ANP Cross-Linking to Cysteine Mutants. The disulfide bonding pattern that was determined for the ECD and partially determined for the truncated receptor led to the hypothesis that the dimeric receptor linkage is mediated by one or both of Cys428 and Cys431. Since the LC-MS data from NPR-C6Δ34 provided only one fragment corresponding to this region of the receptor, we cannot rule out that we had preferentially detected the fragment from the monomeric receptor. However, the participation of Cys residues 63, 91, 168, and 216 in loop formation leaves only 428 and 431 as potential candidates to mediate receptor dimerization. In order to test this interpretation, three full-length receptors were constructed in which either Cys428 or Cys431 alone, or both cysteines together, were replaced by serine using site-directed mutagenesis. The receptors were transiently expressed and identified by autoradiography of gels run after cross-linking with ^{125}I-ANP (Figure 4). The wild-type receptor shows a mixture of monomer and dimer. If either Cys residue is mutated to Ser, there is cross-linking predominantly to dimeric receptor, with much less monomer. When both Cys428 and Cys431 are mutated, only monomeric receptor protein is observed. These results indicate that a dimer can be formed by Cys428–Cys′428 or Cys431–Cys′431 (in the mutants) or Cys428–Cys′431/Cys′428–Cys431 as suggested from the LC-MS data with truncated NPR-C. The close proximity of these two amino acids in the peptide backbone could permit these slightly different linkages to form without noticeably affecting the binding affinity of the receptor for the ligand. Both NPR-C5 and -C6 show very similar kinetics and affinity for ligand binding (Mizuno et al., 1993). The observation of monomeric NPR-C6 suggests that the *intra*molecular disulfide Cys428–Cys431 forms in the wild-type receptor, as observed for the fusion protein-derived ECD. However, the existence of the free thiols for Cys428 and Cys 431 in the wild-type receptor cannot be ruled out on the basis of the data presented here.

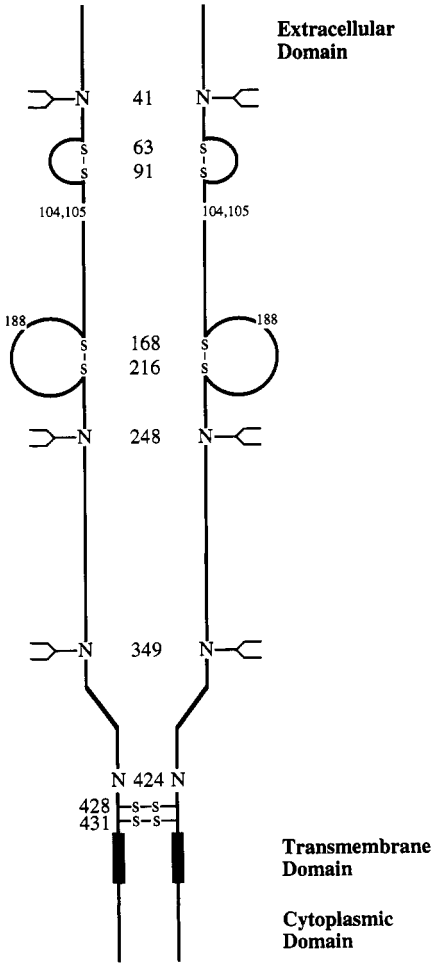

FIGURE 5: Model of the NPR-C homodimer. Disulfide-bonded loops and intermolecular disulfide bonds are indicated by S–S. Occupation of potential N-linked glycosylation sites (N) is indicated by the branch structure. Positions of Cys residues and N-linked sites are indicated by the numbers down the middle of the structure and to the left of the intermolecular disulfide. The carbohydrate classes are based on data from the CHO-derived ECD (N41: complex; N248: high mannose; N349: complex/partial). For simplicity we have not indicated in this model the potential C428–C′431 linkage for the C6 homodimer. Amino acid residues involved in ligand binding (104, 105, 188) are also indicated.

A Disulfide-Bond Model for NPR-C Homodimer. On the basis of our results from LC-MS disulfide mapping and mutagenesis of full-length NPR-C6, we propose a model for the intramolecular and intermolecular linkages of the receptor (Figure 5). This model agrees with recent data on the disulfide map of bovine NPR-C5 (Itakura et al., 1994). Two loops of 29 and 49 amino acids form the intramolecular disulfides in either monomer or dimer, and homodimer formation is mediated by Cys residues immediately adjacent to the membrane. The molecular basis of homodimer formation was demonstrated using NPR-C6 and mutagenesis of Cys428 and Cys431. Since Cys428 is conserved in NPR-C5, we suggest that this residue is responsible for dimer formation with this variant of NPR-C. In our model we have illustrated one possibility for dimer formation, although our results indicate that Cys428–Cys′431, and Cys′428–Cys431 linkages may form. The glycosylation sites based on the mammalian-derived ECD molecule are shown. Three of the four potential N-linked sites are occupied, two with complex carbohydrate, Asn41 and Asn349, and one with high-mannose oligosaccharide, Asn248. A detectable portion of the receptor does not have modification of Asn349, and Asn424 was not modified at all. Our results are consistent with those of Porter et al. (1989), who found using glycosidases that both complex and high-mannose sugars are present on soluble bovine NPR-C5 ECD.

Expression and purification of full-length and the Δ34 truncation mutant of NPR-C6 demonstrate that dimer formation is not predicated on the presence of the cytoplasmic domain. In contrast, Porter et al. (1989) have shown that soluble ECD for bovine NPR-C5 is secreted as a monomer. It thus appears that membrane association is required for homodimer formation; however, we do not know if membrane association per se is sufficient, or if the native transmembrane domain of NPR-C is required. Alternatively, dimerization could result from a slow reaction on the membrane that is dependent more on the local concentration of receptor than on specific compartmentalization or transmembrane domain amino acid sequences. In this scenario the orientation of the subunits would be important since we found that the ECD derived from the forced dimer C-IgG was a monomer on a nonreduced gel, with Cys428–Cys431 intramolecular disulfide linkage determined by LC-MS.

Two recent reports have described residues that are involved in ANP binding to NPR-C. Iwashina et al. (1994) identified H104 and W105, two amino acids that are invariant among all known NPR sequences, as essential for ligand binding to bovine NPR-C5. Using rat and human NPR-C6, Engel et al. (1994) identified position 188 as important in modulating the species-specific pharmacology of the receptor. The first and second sites, positions 104 and 105, are just outside the first disulfide loop, and the third site, position 188, is within the second loop (Figure 5).

Conserved Cysteine Residues in Other NPR's. For the three members of the natriuretic peptide receptor family,

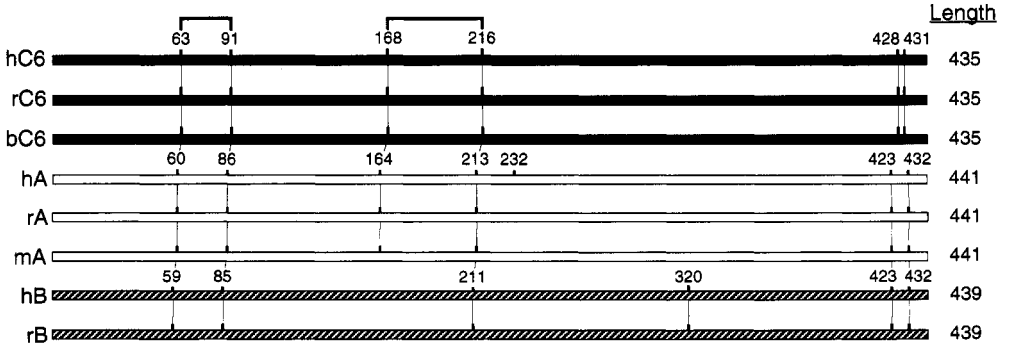

FIGURE 6: Homology alignment of Cys residues for NPR's. The intramolecular disulfide linkages of human NPR-C6 are indicated across the top with Cys residues in alignment to NPR-C, NPR-A, and NPR-B from among human (h), bovine (b), rat (r), and mouse (m). Conserved Cys residues based on amino acid sequence similarity are connected by vertical lines. The last two Cys residues in NPR-C do not align with the last two Cys residues of NPR-A and NPR-B. The total length of each ECD, in amino acids, is shown at the right.

sequence homology is reflected in the conserved location of some, but not all, Cys residues (Figure 6). For human (Lowe et al., 1990; Porter et al., 1990), rat (Engel et al., 1994), and bovine (Fuller et al., 1988; Mizuno et al., 1993) NPR-C, there is greater than 95% sequence identity, including conservation of Cys residues. For both human and bovine NPR-C, C5 and C6 versions have been described, and only NPR-C6 has been described so far for the rat. We expect that the two disulfide-bonded loops we have described for hNPR-C6 will also be present in this receptor from different species, with homodimer formation mediated via the juxtamembrane Cys residue or residues. Mizuno et al. (1993) have studied the cross-linking of ^{125}I-ANP to NPR-C5 and NPR-C6 and found that the dimeric form of NPR-C6 does not cross-link ligand as efficiently as NPR-C5. One possible explanation for this difference may be the different connectivity between subunits of the dimer in C5 versus C6, whereas our data suggest that Cys428 is linked to Cys'431. In C5 the dimer linkage is Cys428–Cys'428 (Itakura et al., 1994). The different linkages may in fact result in a slightly different quaternary structure for the dimer which is reflected in the differing cross-linking efficiencies. Despite these differences between NPR-C5 and -C6, they bind ligand in nearly identical fashion (Mizuno et al., 1993).

For several species of NPR-A, the cysteine residues forming the two disulfide-bonded loops in NPR-C are conserved (Figure 6). For NPR-A there are six Cys residues conserved among human (Lowe et al., 1989), rat (Chinkers et al., 1989), and mouse (Pandey & Singh, 1990) sequences. Human NPR-A is the only one of the three with a seventh Cys residue, at position 232 (Figure 6). No conclusion can be drawn concerning the disulfide bonding of the two Cys residues of NPR-A at positions 423 and 432 near the membrane, since these are not in a region of high sequence similarity with NPR-C.

NPR-B has Cys residues at 59 and 85 corresponding to those forming the first NPR-C loop (Figure 6). Cys211 of NPR-B is homologous to Cys216 forming the second larger loop in NPR-C; however, the analogous first residue for this loop is missing. This position may have been replaced by Cys320, found in both human (Chang et al., 1989) and rat (Schulz et al., 1989) NPR-B. If Cys211 of NPR-B is forming an intramolecular disulfide bond, then we suggest the most likely candidate for pairing is Cys320. The juxtamembrane Cys residues for NPR-B are conserved with NPR-A, suggesting a distinct disulfide structure for the guanylyl cyclase extracellular domains in this region compared to NPR-C.

The data we have presented on the disulfide bonding of NPR-C have allowed the construction of a model for the intra- and intermolecular connectivity of the Cys–Cys linkages. In addition, our results suggest a model for the disulfide bonding pattern of the receptor guanylyl cyclases. The first disulfide loop of NPR-C may be conserved in both NPR-A and NPR-B, whereas the second loop may be in NPR-A only. It is worth noting that the first loop (NPR-C residues 63–91) overlaps with the region of highest sequence similarity among these three receptors (Chang et al., 1989). Overall, there is from 30% to 33% amino acid sequence identity among the three ECD's; however, the region from 83 to 114 (NPR-C numbering) is 71–79% identical between these receptors. This region may thus represent a conserved structural motif in all three types of NPR. Our results provide a basis for further studies on the structure and function of natriuretic peptide receptors.

ACKNOWLEDGMENT

The authors thank Thomas Stapp and Lisa Graham for providing the purified C-IgG, Rich Laura for initial cleavage and purification of the ECD, Jim Bourell for assistance with the LC-MS, Bill Henzel and Chris Grimley for peptide sequencing, Mike Mulkerrin for suggestions on the lower pH tryptic digestion conditions, Josh Theaker for the MAPMASS program, Beth Gillece-Castro for discussions on glycosylation, and Mark Sliwkowski for discussions on receptor purification.

REFERENCES

Aburaya, M., Minamino, N., Hino, J., Kangawa, K., & Matsuo, H. (1989) *Biochem. Biophys. Res. Commun. 165*, 880–887.
Anand-Srivastava, M., Sairam, M. R., & Cantin, M. (1990) *J. Biol. Chem. 265*, 8566–8572.
Bennett, B. D., Bennett, G. L., Vitangcol, R. V., Jewett, J. R. S., Burnier, J., Henzel, W., & Lowe, D. G. (1991) *J. Biol. Chem. 266*, 23060–23067.
Blomback, B (1967) *Methods Enzymol. 11*, 398–413.
Brenner, B. M., Ballermann, B. J., Gunning, M. E., & Zeidel, M. L. (1990) *Physiol. Rev. 70*, 665–699.
Bruins, A. P., Covey, T. R., & Henion, J. D. (1987) *Anal. Chem. 59*, 2642–2646.
Carr, S. A., & Roberts, G. D. (1986) *Anal. Biochem. 157*, 396–406.
Carr, S. A., Hemling, M. E., Bean, M. F., & Roberts, G. D. (1991) *Anal. Chem. 63*, 2802–2824.
Chamow, S. M., Peers, D. H., Byrn, R. A., Mulkerrin, M. G., Harris, R. J., Wang, W.-C., Bjorkman, P. J., Capon, D. J., & Ashkenazi, A. (1990) *Biochemistry 29*, 9885–9891.
Chang, M. S., Lowe, D. G., Lewis, M., Hellmiss, R., Chen, E., & Goeddel, D. V. (1989) *Nature 341*, 68–72.
Chinkers, M., Garbers, D. L., Chang, M.-S., Lowe, D. G., Chin, H., Goeddel, D.V., & Schulz, S. (1989) *Nature 338*, 78–83.
Clavell, A. L., Stingo, A. J., Wei, C. M., Heublein, D. M., & Burnett, J. C. (1993) *Am. J. Physiol. 264*, R290–R295.
Conboy, J. T., & Henion, J. D. (1992) *J. Am. Soc. Mass Spectrom. 3*, 804–814.
Drewett, J. G., Zeigler, R. J., & Trachte, G. J. (1992) *J. Pharm. Exp. Ther. 260*, 689–696.
Duffin, K. L., Welply, J. K., Huang, E., & Henion, J. D. (1992) *Anal. Chem. 64*, 1440–1448.
Engel, A. M., Schoenfeld, J. R., & Lowe, D. G. (1994) *J. Biol. Chem. 269*, 17005–17008.
Fenn, J. B., Mann, M., Meng, C. K., Wong, S. F., & Whitehouse, C. M. (1989) *Science 246*, 64–71.
Fuller, F., Porter, J. G., Arfsten, A. E., Miller, J., Schilling, J. W., Scarborough, R. M., Lewicki, J. A., & Schenck, D. B. (1988) *J. Biol. Chem. 263*, 9395–9401.
Gall, W. E., Cunningham, B. A., Waxdal, M. J., Konigsberg, W. H., & Edelman, G.M. (1968) *Biochemistry 7*, 1973–1982.
Goochee, C. F., Gramer, M. J., Andersen, D. C., Bahr, J. B, & Rasmussen, J. R. (1991) *Bio/Technology 9*, 1347–1355.
Gorman, C. M., Gies, D. R., & McCray, G. (1990) *DNA Protein Eng. Tech. 2*, 3–10.
Henzel, W. J., Bourell, J. H., & Stults, J. T. (1990) *Anal. Biochem. 187*, 228–233.
Hirata, M., Chang, C. H., & Murad, F. (1989) *Biochim. Biophys. Acta 1010*, 346–351.
Huddleston, M. J., Bean, M. F., & Carr, S. A. (1993) *Anal. Chem. 65*, 877–884.
Itakura, M., Iwashina, M., Mizuno, T., Ito, T., Hagiwara, H., & Hirose, S. (1994) *J. Biol. Chem. 269*, 8314–8318.
Iwashina, M., Mizuno, T., Hirose, S., Ito, T., & Hagiwara, H. (1994) *J. Biol. Chem. 115*, 563–567.
Johnson, R. S., Martin, S. A., Biemann, K., Stults, J. T., & Watson, J. T. (1987) *Anal. Chem. 59*, 2621–2625.
Kitts, P. A., Ayres, M. D., & Possee, R. D. (1990) *Nucleic Acids Res. 18*, 5667–5672.

Koller, K. J., Lowe, D. G., Bennett, G. L., Minamino, N., Kangawa, K., Matsuo, H., & Goeddel, D. V. (1991) *Science 252*, 120–123.
Kunkel, T. A. (1985) *Proc. Natl. Acad. Sci. U.S.A. 82*, 488.
Levin, E. R. (1993) *Endocrinol. Metab. 27*, E483–E489.
Ling, V., Guzzetta, A. W., Canova-Davis, E., Stults, J. T., Hancock, W. S., Covey, T. R., & Shushan, B. I. (1991) *Anal. Chem. 63*, 2909–2915.
Lowe, D. G., Chang, M.-S., Hellmiss, R., Chen, E., Singh, S., Garbers, D. L., & Goeddel, D. V. (1989) *EMBO J. 8*, 1377–1384.
Lowe, D. G., Camerato, T. R., & Goeddel, D. V. (1990) *Nucleic Acids Res. 18*, 3412.
Maack, T., Okolicany, J., Koh, G. Y., & Price, D. A. (1993) *Sem. Nephrol. 13*, 50–60.
Manneberg, M., Friedlein, A., Kurth, H., Lahm, H.-W., & Fountoulakis, M. (1994) *Protein Sci. 3*, 30–38.
Matsudaira, P. (1987) *J. Biol. Chem. 262*, 10035–10038.
Meloche, S., McNicoll, N., Liu, B., Ong, H., & De Lean, A. (1988) *Biochemistry 27*, 8151–8158.
Mizuno, T., IwashiNa, M., Itakura, M., Hagiwara, H., & Hirose, S. (1993) *J. Biol. Chem. 268*, 5162–5167.
Morris, H. R., & Pucci, P. (1985) *Biochem. Biophys. Res. Commun. 126*, 1122–1128.
Mukoyama, M., Nakao, K., Hosoda, K., Suga, S., Saito, Y., Ogawa, Y., Kambayashi, Y., Inouye, K., & Imura, H. (1991) *J. Clin. Invest. 87*, 1402–1412.
Nussenzveig, D. R., Lewicki, J. A., & Maack, T. (1990) *J. Biol. Chem. 265*, 20952–20958.
Pandey, K., & Singh, S. (1990) *J. Biol. Chem. 265*, 12342–12348.
Porter, J. G., Wang, Y., Schwartz, K., Arfsten, A., Loffredo, A., Spratt, K., Schenk, D. B., Fuller, F., Scarborough, R. M., & Lewicki, J. A. (1988) *J. Biol. Chem. 263*, 18827–18833.
Porter, J. G., Scarborough, R. M., Wang, Y., Schenk, D., McEnroe, G. A., Kang, L.-L., & Lewicki, J. A. (1989) *J. Biol. Chem. 264*, 14179–14184.
Porter, J. G., Arfsten, A., Fuller, F., Miller, J. A., Gregory, L. C., & Lewicki, J. A. (1990) *Biochem. Biophys. Res. Commun. 171*, 796–803.
Possee, R. D., & Howard, S. C. (1987) *Nucleic Acids Res. 15*, 10233–10248.
Ruskoaho, H. (1993) *Pharmacol. Rev. 44*, 479–602.
Saheki, T., Mizuno, T., Iwata, T., Saito, Y., Nagasawa, T., Mizuno, K. U., Ito, F., Ito, T., Hagiwara, H., & Hirose, S. (1991) *J. Biol. Chem. 266*, 11122–11125.
Schenk, D. B., Phelps, M. N., Porter, J. G., Fuller, F., Cordell, B., & Lewicki, J. A. (1987) *Proc. Natl. Acad. Sci. U.S.A. 84*, 1521–1525.
Schindler, P. A., VanDorsselaer, A., & Falick, A. M. (1993) *Anal. Biochem. 213*, 256–263.
Schulz, S., Singh, S., Bellet, R. A., Singh, G., Tubb, D. J., Chin, H., & Garbers, D. L. (1989) *Cell 59*, 1155–1162.
Shimonaka, M., Saheki, T., Hagiwara, H., Ishido, M., Nogi, A., Fujita, J., Wakita, K., Inada, Y., Kondo, J., & Hirose, S. (1987) *J. Biol. Chem. 262*, 5510–5519.
Spellman, M. W., Basa, L. J., Leonard, C. K., Chakel, J. A., O'Connor, J. V., Wilson, S., & van Halbeek, H. (1989) *J. Biol. Chem. 264*, 14100–14111.
Stingo, A. J., Clavell, A. L., Aarhus, L. L., & Burnett, J. C. (1992) *Am. J. Physiol. 262*, H308–H312.
Sudoh, T., Kangawa, K., Minamino, N., & Matsuo, H. (1988) *Nature 332*, 78–81.
Sudoh, T., Minamino, N., Kangawa,, K., & Matsou, H. (1990) *Biochem. Biophys. Res. Commun. 168*, 863–870.
Suga, S., Nakao, K., Itoh, H., Komatsu, Y., Ogawa, Y., Hama, N., & Imura, H. (1992a) *J. Clin. Invest. 90*, 1145–1190.
Suga, S., Nakao, K., Hosada, K., Mukoyama, M., Oawa, Y., Shirakami, G., Arai, H., Saito, Y., Kambayashi, Y., Inouye, K., & Imura, H. (1992b) *Endocrinology 130*, 2229–2239.
Tan, A. C. I. T. L., Russel, F. G. M., Thien, T., & Benraad, T. J. (1993) *Clin. Pharmacokinet. 24*, 28–45.
Yamaguchi, M., Rutledge, L. J., & Garbers, D. L. (1990) *J. Biol. Chem. 265*, 20414–20420.